2 The two dimensional cutting theory

One of the strong non-linear effects in the equilibrium equations of motion for the determination of the cutter-suction and cutter-wheel dredger motions, is the interaction between the excavating element and the soil. A good description of the cutting process is essential for a reliable simulation of the ship motions, in order to be able to predict the usability and the design of sea-going dredging vessels.

Although calculation models for the determination of the cutting forces for dry sand were available for a long time (Hettiaratchi & Reece [20,21,22,23,24,66], Hatamura & Chiiwa [18] etc.) it is only since the seventies and the eighties that the cutting process in saturated sand is extensively researched at the Waterloopkundig Laboratorium in Delft (WL, CSB), at the Technische Hogeschool in Delft and at the Mineraal Technologisch Instituut (MTI, IHC).

First the process is described, for a good understanding of the terminology used in the literature discussion.

2.1 Description of the process

From literature it is known that, during the cutting process, the sand increases in volume (see figure 2.1).

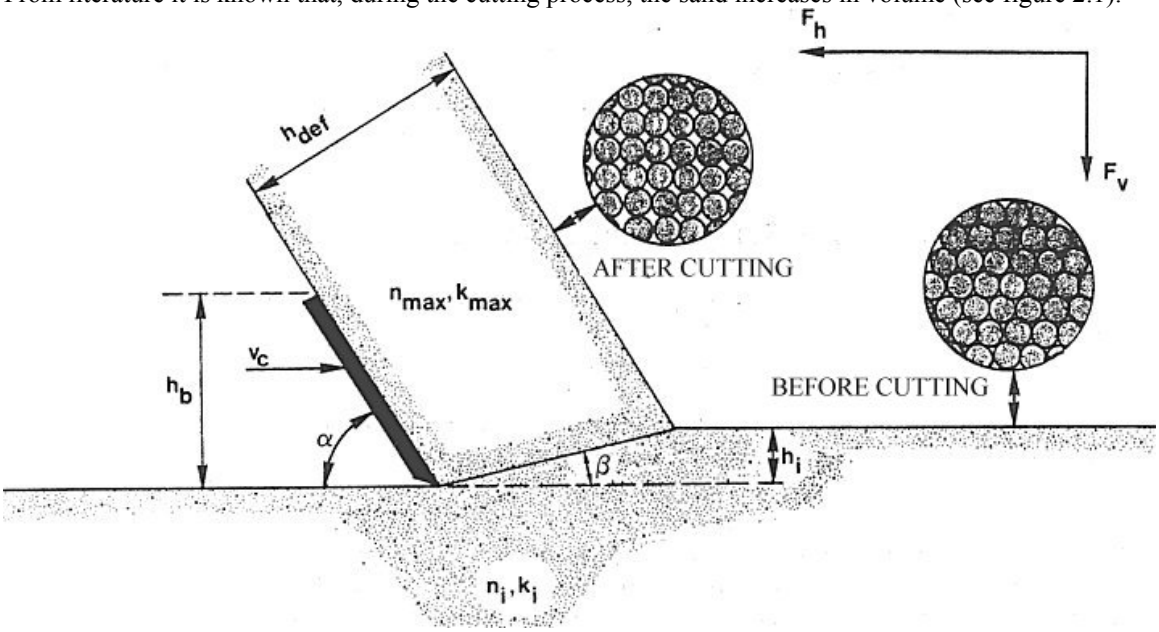

Figure 2-1 The cutting process modeled as a continuous process.

This increase in volume is accredited to dilatancy. This is the change of the pore volume as a result of shear in the sand package. This increase of the pore volume has to be filled with water. The flowing water experiences a certain resistance, which causes sub-pressure in the pore water in the sand package. As a result the grain stresses increase and therefore the needed cutting forces. The speed of the increase of the pore volume in the dilatancy zone, the volume strain rate, is proportional to the cutting velocity. If the volume strain rate is high, there is a chance that the pore pressure reaches the saturated vapor pressure and cavitation occurs. A further increasing volume strain rate will not be able to cause a further decrease of the pore pressure. This also implies that, with a further increasing cutting velocity, the cutting forces cannot increase as a result of the dilatancy properties of the sand. The cutting forces can, however, still increase with an increasing cutting velocity as a result of the inertia forces and the flow resistance.

The cutting process can be subdivided in 5 areas in relation with the cutting forces:

1. Very low cutting velocities, a quasi static cutting process. The cutting forces are determined by the gravitation, cohesion and adhesion.

2. The volume strain rate is high in relation to the permeability of the sand. The volume strain rate is however so small that inertia forces can be neglected. The cutting forces are dominated by the dilatancy properties of the sand.

3. A transition region, with local cavitation. With an increasing volume strain rate, the cavitation area will increase so that the cutting forces increase slightly as a result of dilatancy.

4. Cavitation occurs almost everywhere around and on the blade. The cutting forces do not increase anymore as a result of the dilatancy properties of the sand.

5. Very high cutting velocities. The inertia forces part in the total cutting forces can no longer be neglected but form a substantial part.

2.2 Cutting theory literature

In the seventies extensive research is done on the forces that occur while cutting sand under water. A conclusive cutting theory has however not been published in this period. However qualitative relations have been derived by several researchers, with which the dependability of the cutting forces with the soil properties and the blade geometry are described (Joanknecht [27], van Os [62,63]).
Afterwards it turned out that, in non-published reports for the confidential research program CSB, as indicated in the reference list of [40], Van Os had already developed the basic theory for the cutting of saturated packed sand. Ahead of the real publication [40] is provided by the Waterloopkundig Laboratorium in August 1986.

A process that has a lot of similarities with the cutting of sand as far as water pressure development is concerned, is the, with uniform velocity, forward moving breach. Meijer and van Os [41] 1976 and Meijer [42,43] 1981/1985 have transformed the storage equation for the, with the breach, forward moving coordinate system.

$$\left|\frac{\partial^2 p}{\partial x^2}\right| + \left|\frac{\partial^2 p}{\partial y^2}\right| = \frac{\rho_w \cdot g \cdot v_c}{k} \cdot \left|\frac{\partial e}{\partial x}\right| - \frac{\rho_w \cdot g}{k} \cdot \left|\frac{\partial e}{\partial t}\right| \tag{2.1}$$

In case of a stationary process, the second term on the right is zero, resulting:

$$\left|\frac{\partial^2 p}{\partial x^2}\right| + \left|\frac{\partial^2 p}{\partial y^2}\right| = \frac{\rho_w \cdot g \cdot v_c}{k} \cdot \left|\frac{\partial e}{\partial x}\right| \tag{2.2}$$

Van Os [62,63] 1977 describes the basic principles of the cutting process, with special attention for the determination of the water sub-pressures and the cavitation. Van Os uses the non-transformed storage equation for the determination of the water sub-pressures.

$$\left|\frac{\partial^2 p}{\partial x^2}\right| + \left|\frac{\partial^2 p}{\partial y^2}\right| = \frac{\rho_w \cdot g}{k} \cdot \left|\frac{\partial e}{\partial t}\right| \tag{2.3}$$

The average volume strain rate has to be substituted in the term $\partial e/\partial t$ on the right. The average volume strain rate is the product of the average volume strain of the sand package and the cutting velocity and arises from the volume balance over the shear zone. Van Os gives a qualitative relation between the water sub-pressures and the average volume strain rate:

$$p :: \frac{v_c \cdot h_i \cdot e}{k} \tag{2.4}$$

The problem of the solution of the storage equation for the cutting of sand under water is a mixed boundary-value problem, for which the water sub-pressures along the boundaries are known (hydrostatic).

Joanknecht [26,27] 1973 assumes that the cutting forces are determined by the sub-pressure in the sand package. A distinction is made between the parts of the cutting force caused by the inertia forces, the sub-pressure behind the blade and the soil mechanical properties of the sand. The influence of the geometrical parameters gives the following qualitative relation:

$$F_{ci} :: v_c \cdot h_i^2 \cdot b \tag{2.5}$$

The cutting force is proportional to the cutting velocity, the blade width and the square of the initial layer-thickness. A relation with the pore percentage and the permeability is also mentioned. A relation between the cutting force and these soil mechanical properties is however not given. It is observed that the cutting forces increase with an increasing blade angle.

In the eighties research has led to more quantitative relations. In 1984 Van Leussen and Nieuwenhuis [39] discuss the soil mechanical aspects of the cutting process. The forces models of Miedema [54,57] and Steeghs [72,73] are published 1985/86, while the CSB (Combinatie Speurwerk Baggertechniek) model (van Leussen en van Os [40]), however developed in the early seventies at the Waterloopkundig Laboratorium (van Os [62,63]), will be published in 1987.

Brakel [5] 1982 derives a relation for the determination of the water sub-pressures based upon, over each other rolling, round grains in the shear zone. The force part resulting from this is added to the model of Hettiaratchi and Reece [23].

Miedema [52] 1983 has combined the qualitative relations of Joanknecht [26,27] and Van Os [62,63] to the following relation:

$$F_{ci} :: \frac{\rho_w \cdot g \cdot v_c \cdot h_i^2 \cdot b \cdot e}{k} \tag{2.6}$$

With this basic equation calculation models are developed for a cutterhead and for the periodical moving cutterhead in the breach. The proportionality constants are determined empirically. The soil module of the DREDMO program is also developed from these models (Miedema [36,47]). This will be discussed in the appropriate chapters.

Van Leussen and Nieuwenhuis [39] 1984 discuss the soil mechanical aspects of the cutting process. Important in the cutting process is the way shear takes place and the shape or angle of the shear plane, respectively shear zone. In literature no unambiguous image could be found. Cutting tests along a windowpane gave an image in which the shape of the shear plane was more in accordance with the so-called "stress characteristics" than with the so-called "zero-extension lines". Therefore, for the calculation of the cutting forces, the "stress characteristics method" is used (Mohr-Coulomb failure criterion). For the calculation of the water sub-pressures, however, the "zero-extension lines" are used, which are lines with a zero linear strain. A closer description has not been given for both calculations.

Although the cutting process is considered as being two-dimensional, Van Leussen and Nieuwenhuis found, that the angle of internal friction, measured at low deformation rates in a triaxial apparatus, proved to be sufficient for dredging processes. Although the cutting process can be considered as a two-dimensional process and therefore it should be expected that the angle of internal friction has to be determined with a "plane deformation test". A sufficient explanation has not been found.

Little is known about the value of the angle of friction between sand and steel. Van Leussen and Nieuwenhuis don't give an unambiguous method to determine this soil mechanical parameter. It is, however, remarked that at low cutting velocities (0.05 mm/s), the soil/steel angle of friction can have a statistical value which is 1.5 to 2 times larger than the dynamic soil/steel angle of friction. The influence of the initial density on the resulting angle of friction is not clearly present, because loose packed sand moves over the blade. The angles of friction measured on the blades are much larger than the angles of friction measured with an adhesion cell, while also a dependency with the blade angle is observed.

With regard to the permeability of the sand, Van Leussen and Nieuwenhuis found that no large deviations of Darcy's law occur with the water flow through the pores. The found deviations are in general smaller than the accuracy with which the permeability can be determined in situ.

The size of the area where $\partial e/\partial t$ from equation (2.5) is zero can be clarified by the figures published by Van Leussen and Nieuwenhuis. The basis is formed by a cutting process where the density of the sand is

increased in a shear band with a certain width. The undisturbed sand has the initial density while the sand after passage of the shear band possesses a critical density. This critical density appeared to be in good accordance with the wet critical density of the used types of sand. This implies that outside the shear band the following equation is valid:

$$\left|\frac{\partial^2 p}{\partial x^2}\right| + \left|\frac{\partial^2 p}{\partial y^2}\right| = 0 \qquad (2.7)$$

Values for the various densities are given for three types of sand. Differentiation of the residual density as a function of the blade angle is not given. A verification of the water pressures calculations is given for a 60° blade with a blade-height/layer-thickness ratio of 1.

Miedema [51,52] 1984 gives a formulation for the determination of the water sub-pressures. The deformation rate is determined by taking the volume balance over the shear zone, as Van Os [62,63] did. The deformation rate is modeled as a boundary condition in the shear zone , while the shear zone is modeled as a straight line instead of a shear band as with Van Os [62,63] and Van Leussen and Nieuwenhuis [39]. The influence of the water depth on the cutting forces is clarified. Also explained are the forces on the cutterhead on the basis of equation (2.6) and a survey is given of the possibilities of DREDMO.
Steeghs [72] 1985 developed a theory for the determination of the volume strain rate, based upon a cyclic deformation of the sand in a shear band. This implies that not an average value is taken for the volume strain rate but a cyclic, with time varying, value, based upon the dilatancy angle theory.

Miedema [54,55] 1985 derives equations for the determination of the water sub-pressures and the cutting forces, based upon [46,51,52]. The water sub-pressures are determined with a finite element method. Explained are the influence of the permeability of the disturbed and undisturbed sand and the determination of the shear angle. The derived theory is verified with model tests. On basis of this research n_{max} is chosen for the residual pore percentage instead of the wet critical density.

Steeghs [72,73] 1985/1986 derives equations for the determination of the water sub-pressures according an analytical approximation method. With this approximation method the water sub-pressures are determined with a modification of equation (2.4) derived by Van Os [62,63] and the storage equation (2.7). Explained is how cutting forces can be determined with the force equilibrium on the cut layer. Also included are the gravity force, the inertia forces and the sub-pressure behind the blade. For the last influence factor no formulation is given. Discussed is the determination of the shear angle. Some examples of the cutting forces are given as a function of the cutting velocity, the water depth and the sub-pressure behind the blade. A verification of this theory is not given.

Miedema [56] 1986 develops a calculation model for the determination of the cutting forces on a cutter-wheel based upon [54,55]. This will be discussed in the appropriate section. Also nomograms are published with which the cutting forces and the shear angle can be determined in a simple way. Explained is the determination of the weighted average permeability from the permeability of the disturbed and undisturbed sand. Based upon the calculations it is concluded that the average permeability forms a good estimation.

Miedema [57] 1986 extends the theory with adhesion, cohesion, inertia forces, gravity, and sub-pressure behind the blade. The method for the calculation of the coefficients for the determination of a weighed average permeability are discussed. It is concluded that the additions to the theory lead to a better correlation with the tests results.

Van Os and Van Leussen [40] 1986 summarize the publications of Van Os [62,63] and of Van Leussen and Nieuwenhuis [39] and give a formulation of the theory developed in the early seventies at the Waterloopkundig Laboratorium. Discussed are the water pressures calculation, cavitation, the weighed average permeability, the angle of internal friction, the soil/steel angle of friction, the permeability, the volume strain and the cutting forces. Verification is given of a water pressures calculation and the cutting

forces. The water sub-pressures are determined with equation (2.4) derived by Van Os [62,63]. The water pressures calculation is performed with the finite difference method, in which the height of the shear band is equal to the mesh width of the grid. The size of this mesh width is considered to be arbitrary. From an example, however, it can be seen that the shear band has a width of 13% of the layer-thickness. Discussed is the determination of a weighed average permeability. The forces are determined with Coulomb's method.

2.3 Determination of the sub-pressure around the blade

The cutting process can be modeled as a two-dimensional process, in which a straight blade cuts a small layer of sand (figure 2.1). The sand is deformed in the shear zone, also called deformation zone or dilatancy zone. During this deformation the volume of the sand changes as a result of the shear stresses in the shear zone. In soil mechanics this phenomenon is called dilatancy. In firm packed sand the pore volume is increased as a result of the shear stresses in the deformation zone. This increase in the pore volume is thought to be concentrated in the deformation zone, with the deformation zone modeled as a straight line (line sink). Water has to flow to the deformation zone to fill up the increase of the pore volume in this zone. As a result of this water flow the grain stresses increase and the water pressures decrease. Therefore there are water sub-pressures.

This implies that the forces necessary for cutting firm packed sand under water will be determined for an important part by the dilatancy properties of the sand. At low cutting velocities these cutting forces are also determined by the gravity, the cohesion and the adhesion for as far as these last two soil mechanical parameters are present in the sand. Is the cutting at high velocities than the inertia forces will have an important part in the total cutting forces.

If the cutting process is assumed to be stationary, the water flow through the pores of the sand can be described in a blade motions related coordinate system. The determination of the water sub-pressures in the sand around the blade is then limited to a mixed boundary conditions problem. The potential theory can be used to solve this problem. For the determination of the water sub-pressures it is necessary to have a proper formulation of the boundary condition in the shear zone. Miedema [52] 1984 derived the basic equation for this boundary condition.
In 1985 [54,55] and 1986 [57] a more extensive derivation is published.

If it is assumed that no deformations take place outside the deformation zone, then:

$$\left|\frac{\partial^2 p}{\partial x^2}\right| + \left|\frac{\partial^2 p}{\partial y^2}\right| = 0 \tag{2.8}$$

applies for the sand package around the blade.

The boundary condition is in fact a specific flow rate (fig. 2.2) that can be determined with the following hypothesis.

For a sand element in the deformation zone, the increase in the pore volume per unit of blade length, is:

$$\Delta V = e \cdot \Delta A = e \cdot \Delta x \cdot \Delta h_i = e \cdot \Delta x \cdot \Delta l \cdot \sin(\beta) \tag{2.9}$$

In which: $$e = \frac{n_{max} - n_i}{1 - n_{max}} \tag{2.10}$$

For the residual pore percentage is chosen for n_{max} on the basis of the ability to explain the water sub-pressures, measured in the laboratory tests. This is described in chapter 3.

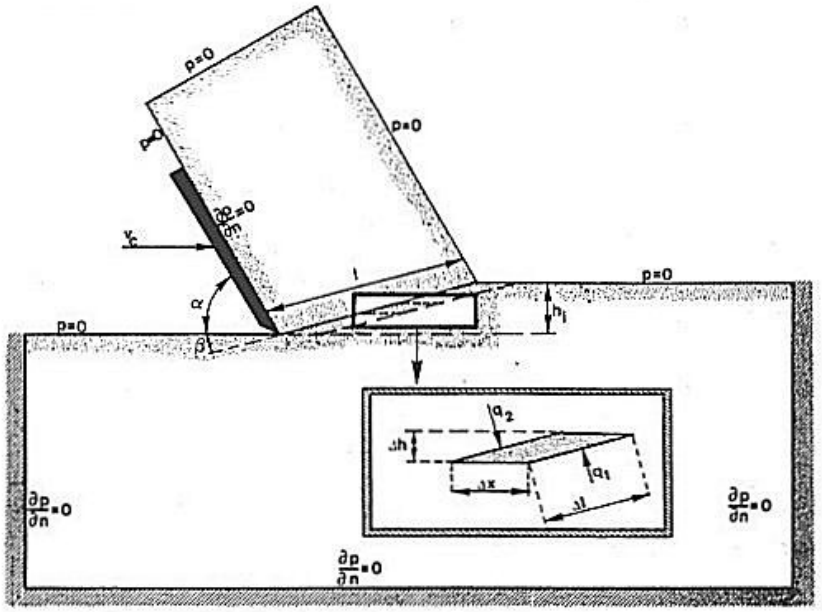

Figure 2-2 The volume balance over the shear zone.

The volume flow rate flowing to the sand element, is equal to:

$$\Delta Q=\frac{\partial V}{\partial t}=e\cdot\frac{\partial x}{\partial t}\cdot\Delta l\cdot\sin(\beta)=e\cdot v_c\cdot\Delta l\cdot\sin(\beta) \tag{2.11}$$

With the aid of Darcy's law the next differential equation can be derived for the specific flow rate. perpendicular to the deformation zone:

$$q=\frac{\partial Q}{\partial l}=q_1+q_2=\frac{k_i}{\rho_w\cdot g}\cdot\left|\frac{\partial p}{\partial n}\right|_1+\frac{k_{max}}{\rho_w\cdot g}\cdot\left|\frac{\partial p}{\partial n}\right|_2=e\cdot v_c\cdot\sin(\beta) \tag{2.12}$$

The partial derivative $\partial p/\partial n$ is the derivative of the water sub-pressures perpendicular on the boundary of the area, in which the water sub-pressures are calculated (in this case the deformation zone). The boundary conditions on the other boundaries of this area are indicated in figure 2.2. A hydrostatic pressure distribution is assumed on the boundaries between sand and water. This pressure distribution equals zero in the calculation of the water sub-pressures, if the height difference over the blade is neglected. The boundaries that form the edges in the sand package are assumed to be impenetrable. This will be further discussed in chapter 2.4.

Making equation (2.12) dimensionless is similar to that of the breach equation of Meijer and Van Os [41]. In the breach problem the length dimensions are normalized by dividing them by the breach height, while in the cutting of sand they are normalized by dividing them by the cut layer thickness.

Equation (2.12) in normalized format:

$$\frac{k_i}{k_{max}}\cdot\left|\frac{\partial p}{\partial n'}\right|_1+\left|\frac{\partial p}{\partial n'}\right|_2=\frac{\rho_w\cdot g\cdot v_c\cdot e\cdot h_i\cdot\sin(\beta)}{k_{max}} \tag{2.13}$$

With: $n' = n/h_i$

This equation is made dimensionless with:

$$\left|\frac{\partial p}{\partial n}\right|' = \frac{\left|\frac{\partial p}{\partial n'}\right|}{\rho_w \cdot g \cdot v_c \cdot e \cdot h_i / k_{max}} \tag{2.14}$$

The accent indicates that a certain variable or partial derivative is dimensionless. The next dimesionless equation is now valid as a boundary condition in the deformation zone:

$$\frac{k_i}{k_{max}} \cdot \left|\frac{\partial p}{\partial n}\right|'_1 + \left|\frac{\partial p}{\partial n}\right|'_2 = \sin(\beta) \tag{2.15}$$

The storage equation also has to be made dimensionless, which results in the next equation :

$$\left|\frac{\partial^2 p}{\partial x^2}\right|' + \left|\frac{\partial^2 p}{\partial y^2}\right|' = 0 \tag{2.16}$$

Because this equation equals zero, it is similar to equation (2.8)

The water sub-pressures distribution in the sand package can now be determined using the storage equation and the boundary conditions. Because the calculation of the water sub-pressures is dimensionless the next transformation has to be performed to determine the real water sub-pressures .

The real water sub-pressures can be determined by integrating the derivative of the water sub-pressures in the direction of a flow line, along a flow line, so:

$$P_{calc} = \int_{s'} \left|\frac{\partial p}{\partial s}\right|' \cdot ds' \quad \text{along a flow line s'} \tag{2.17}$$

This is illustrated in figure 2.3.

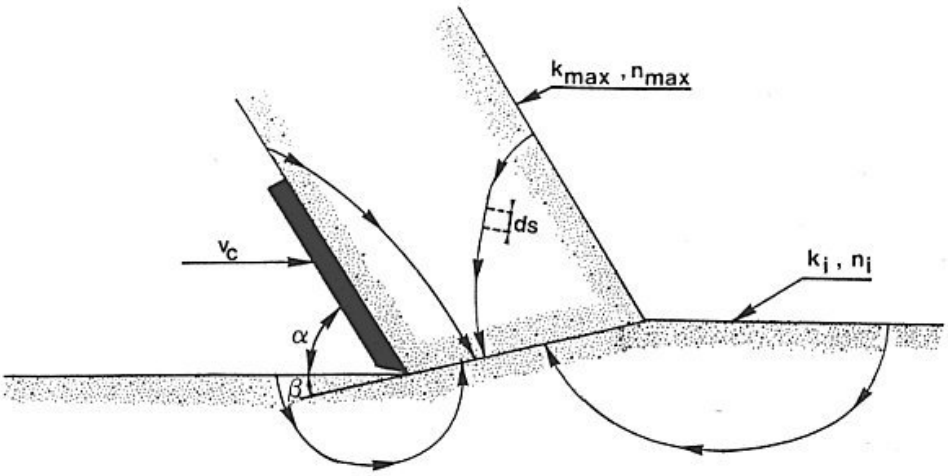

Figure 2-3 Flow of the pore water to the shear zone.

Using equation (2.14) this is written as:

$$P_{werk} = \int_{s} \left|\frac{\partial p}{\partial s}\right| \cdot ds = \int_{s'} \frac{\rho_w \cdot g \cdot v_c \cdot e \cdot h_i}{k_{max}} \cdot \left|\frac{\partial p}{\partial s}\right|' \cdot ds' \qquad (2.18)$$

With: $s' = s/h_i$

This gives the next relation between the really emerging water sub-pressures and the calculated water sub-pressures:

$$P_{werk} = \frac{\rho_w \cdot g \cdot v_c \cdot e \cdot h_i}{k_{max}} \cdot P_{calc} \qquad (2.19)$$

In table 2.1(see appendix B5) the calculated water sub-pressures are listed in relation with the blade angle , the shear angle, the blade-height/layer-thickness ratio and the ratio between the permeability of the disturbed and undisturbed sand. Using equation (2.19) or equation (2.14) also the water sub-pressures, measured in the cutting tests, can be made dimensionless. To be independent of the ratio between the initial permeability k_i and the maximum permeability k_{max} , k_{max} has to be replaced with the weighed average permeability k_m before making the measured water sub-pressures dimensionless. This will be discussed in chapter 2.8.

2.4 Numerical water pressures calculations

The water sub-pressures in the sand package on and around the blade are numerically determined using the finite element method. A standard program package is used (Segal [69]). With the in this package, available "subroutines" a program is written, with which water sub-pressures can be calculated and be output graphically and numerically. The solution of such a calculation is however not only dependent on the physical model of the problem, but also on the next points:

1. The size of the area in which the calculation takes place.
2. The size and distribution of the elements
3. The boundary conditions

The choices for these three points have to be evaluated with the problem that has to be solved in mind. These calculations are about the values and distribution of the water sub-pressures in the shear zone and on the blade. A variation of the values for point 1 and 2 may therefore not influence this part of the solution. This is achieved by on the one hand increasing the area in which the calculations take place in steps and on the other hand by decreasing the element size until the variation in the solution was less than 1%.
The distribution of the elements is chosen such that a finer mesh is present around the blade tip, the shear zone and on the blade, also because of the blade tip problem (chapter 2.5).

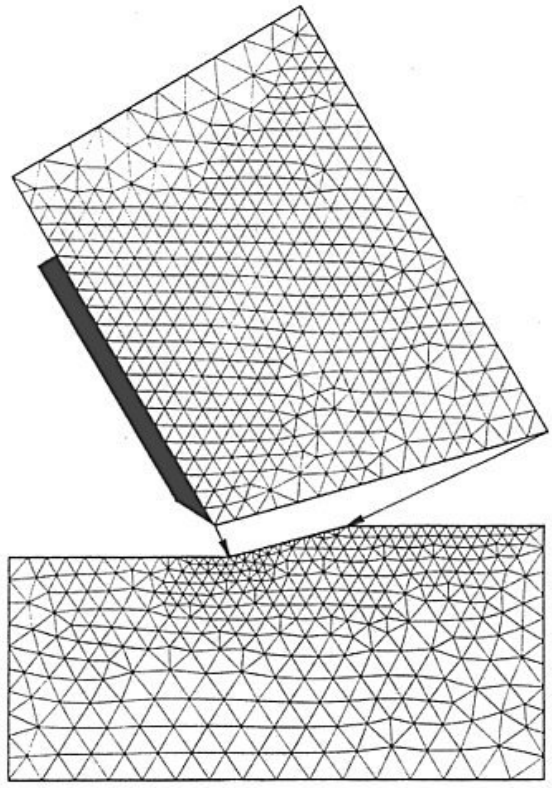

Figure 2-4 The element mesh used in the water pressures calculations.

A number of boundary conditions follow from the physical model of the cutting process, these are:

1. The boundary condition in the shear zone. This is described by equation (2.15).
2. The boundary condition along the free sand surface. The hydrostatic pressure at which the process takes place, can be chosen, when neglecting the dimensions of the blade and the layer in relation to the hydrostatic pressure head. Because these calculations are meant to obtain the difference between the

water sub-pressures and the hydrostatic pressure it is valid to take a zero pressure as the boundary condition.

The boundary conditions along the boundaries of the area where the calculation takes place, that are located in the sand package, are not determined by the physical process. For this boundary condition there is a choice between:

1. A hydrostatic pressure along the boundary.
2. A boundary as an impenetrable wall.
3. A combination of a known pressure and a known specific flow rate.

None of these choices complies with the real process. Water from outside the calculation area will flow through the boundary. This also implies, however, that the pressure along this boundary is not hydrostatic. If, however, the boundary is chosen with enough distance from the real cutting process the boundary condition may not have an influence on the solution. The impenetrable wall is chosen although this choice is arbitrary. Figure 2.2 gives an impression of the size of the area and the boundary conditions, while figure 2.4 shows the element mesh. Figure 2.5 shows the two-dimensional distribution of the water sub-pressures.

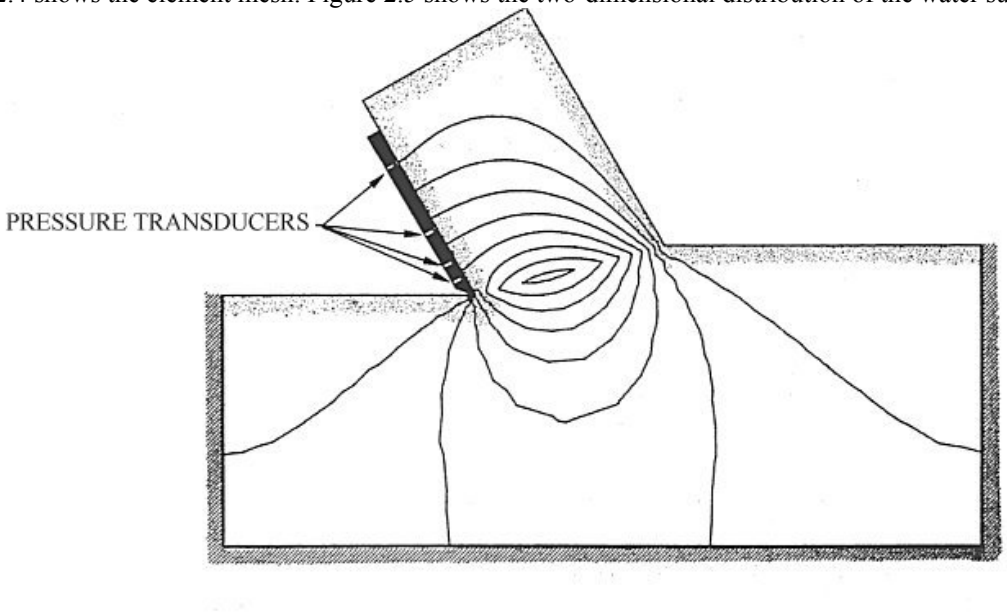

Figure 2-5 The water sub-pressures distribution in the sand package around the blade.

2.5 The blade tip problem

During the physical modeling of the cutting process it has always been assumed that the blade tip is sharp. In other words, that in the numerical calculation, from the blade tip, a hydrostatic pressure can be introduced as the boundary condition along the free sand surface behind the blade. In practice this is never valid, because of the following reasons:

1. The blade tip always has a certain rounding, so that the blade tip can never be considered really sharp.
2. Trough wear of the blade a flat section develops behind the blade tip, which runs against the sand surface (clearance angle ≤ zero)
3. If there is also dilatancy in the sand underneath the blade tip it is possible that the sand runs against the flank after the blade has passed.
4. There will be a certain sub-pressure behind the knife as a result of the blade speed and the cutting process.

A combination of these factors determines the distribution of the water sub-pressures, especially around the blade tip. The first three factors can be accounted for in the numerical calculation as an extra boundary condition behind the blade tip. Along the free sand surface behind the blade tip an impenetrable line element is put in, in the calculation. The length of this line element is varied with $0.0 \cdot h_i$, $0.1 \cdot h_i$ and $0.2 \cdot h_i$. It showed from these calculations that especially the water sub-pressures on the knife are strongly determined by the choice of this boundary condition as indicated in figure 2.6.

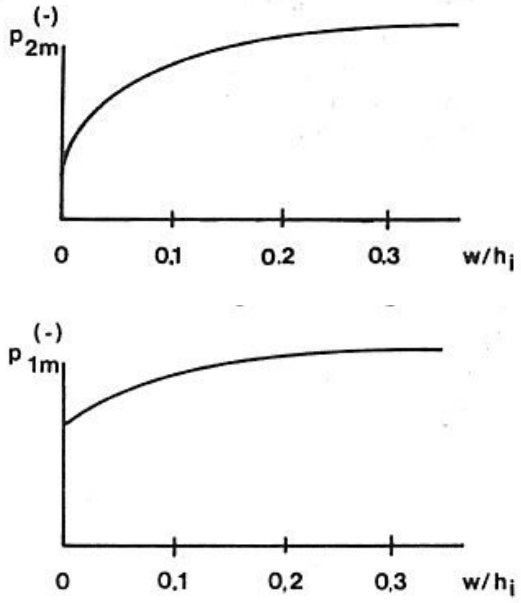

Figure 2-6 a, above: The water sub-pressures distribution on the blade as function of the length of the flat wear section w.
b, below: The water sub-pressures distribution in the shear zone as function of the length of the flat wear section w.

It is hard to estimate to what degree the influence of the sub-pressure behind the blade on the water sub-pressures around the blade tip can be taken into account with these extra boundary condition. Since there is no clear formulation for the sub-pressure behind the blade available, it will be assumed that the extra boundary condition at the blade tip describes this influence. The laboratory research will have to make this more evident.

2.6 The forces on the blade

The forces that act on the blade during the cutting of soil, are transmitted on the blade through grain stresses and water pressures. These forces are caused by:

1. Normal stress, resulting in the force N_2.
2. Shear stress as a result of the soil/steel friction, resulting in S_2.
3. Shear stress as a result of the adhesion between the soil and the blade, resulting in the force A
4. Water sub-pressures on the blade p_{2m}, resulting in the force W_2.
5. Sub-pressure behind the blade p_{3m}, resulting in the force W_3.

These forces are indicated in figure 2.7.

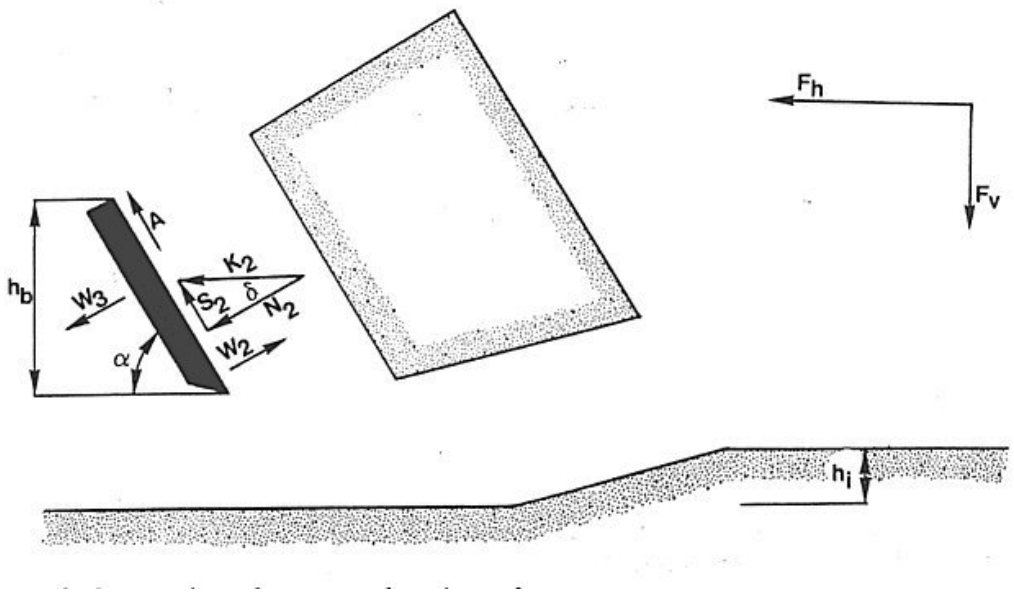

Figure 2-7 The forces on the blade.

The normal force N_2 and the shear force S_2 are related as follows:

$$S_2 = N_2 \cdot \tan(\delta) \qquad K_2 = \sqrt{\left(S_2^2 + N_2^2\right)} \tag{2.20}$$

The resulting water force on the blade W_2 can be determined theoretically (see chapter 2.3). The resulting water force W_3 behind the blade results from measurements and from the determination of the angle of internal friction from measurements (see chapter 3.11). This implies that the resulting grain force K_2 is the only unknown force on the blade. This resulting force can be determined from the force equilibrium on the cut layer according the method of Coulomb [76] extended with the water pressure forces. These forces on the cut layer are shown in figure 2.8. These forces are:

1. The earlier mentioned forces W_2, N_2, S_2 and A.
2. The force W_1 resulting from the water pressures in the shear zone p_{1m}.
3. The force N_1 resulting from the normal stress on the shear zone.
4. The force S_1 resulting from the shear stress as a result of the internal friction of the sand.
5. The force resulting from the cohesion of the sand C.
6. The force as a result of the mass of the sand G.
7. The force as a result of the acceleration of the sand T.
8. The force W_4 as a result of the water resistance.

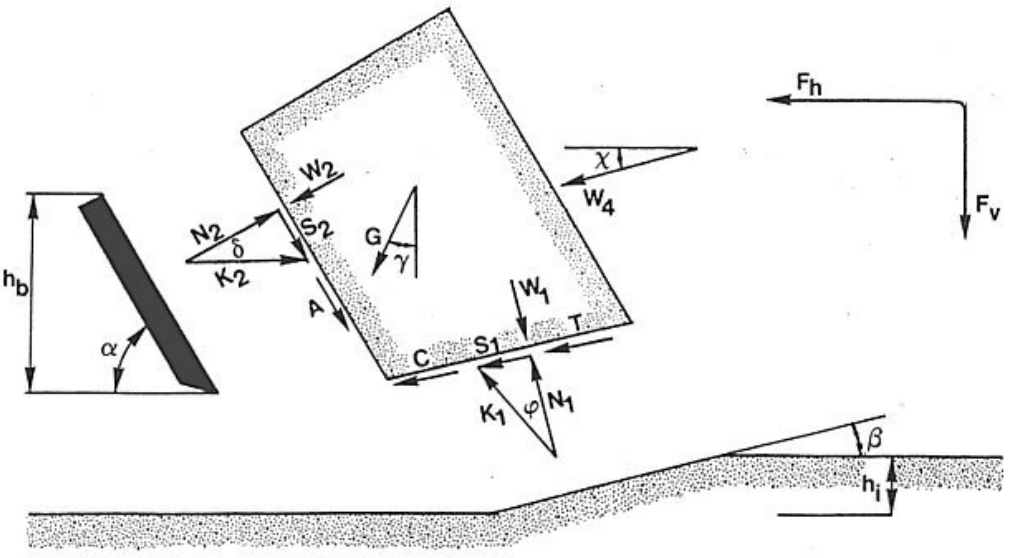

Figure 2-8 The forces acting on the cut layer.

The normal force N_1 and the shear force S_1 are related according:

$$S_1 = N_1 \cdot \tan(\varphi) \qquad K_1 = \sqrt{(S_1^2 + N_1^2)} \tag{2.21}$$

From the horizontal and the vertical force equilibrium on the cut layer, the grain forces K_1 and K_2 can be determined. The horizontal and vertical expressions are related to the direction of the cutting velocity such that the horizontal axis points in the direction of the cutting velocity and the vertical axis is perpendicular to this. This means that the gravity force is not necessarily directed vertically in the figures, but can make an angle γ with the vertical. This is done to ease the determination of the vertical and horizontal equilibrium.

For the horizontal force equilibrium can now be found:

$$\begin{aligned} &K_1 \cdot \sin(\beta+\varphi) - W_1 \cdot \sin(\beta) + C \cdot \cos(\beta) + T \cdot \cos(\beta) + G \cdot \sin(\gamma) + W_4 \cdot \cos(X) \\ &- A \cdot \cos(\alpha) + W_2 \cdot \sin(\alpha) - K_2 \cdot \sin(\alpha+\delta) = 0 \end{aligned} \tag{2.22}$$

And for the vertical force equilibrium can be found:

$$\begin{aligned} &-K_1 \cdot \cos(\beta+\varphi) + W_1 \cdot \cos(\beta) + C \cdot \sin(\beta) + T \cdot \sin(\beta) + G \cdot \cos(\gamma) + W_4 \cdot \sin(X) \\ &+ A \cdot \sin(\alpha) + W_2 \cdot \cos(\alpha) - K_2 \cdot \cos(\alpha+\delta) = 0 \end{aligned} \tag{2.23}$$

For the determination of the forces on the blade only the force K_2 is of importance. For this force can now be derived ($K_2 = K_{21} + K_{22}$):

$$K_{21} = \frac{W_2 \cdot \sin(\alpha+\beta+\varphi) + W_1 \cdot \sin(\varphi)}{\sin(\alpha+\beta+\delta+\varphi)} \tag{2.24}$$

$$K_{22} = \frac{G \cdot \sin(\beta+\varphi+\gamma) + T \cdot \cos(\varphi) + C \cdot \cos(\varphi) - A \cdot \cos(\alpha+\beta+\varphi) + W_4 \cdot \cos(\beta+\varphi-X)}{\sin(\alpha+\beta+\varphi+\delta)} \tag{2.25}$$

The force K_{21} is the water sub-pressures part, while force K_{22} is the part of the gravity, the inertia forces, the cohesion, the adhesion and the water resistance in the force K_2.

The following forces act on the blade:

1. The horizontal force F_h.

$$F_h = -W_2 \cdot \sin(\alpha) + K_2 \cdot \sin(\alpha+\delta) + A \cdot \cos(\alpha) + W_3 \cdot \sin(\alpha) \tag{2.26}$$

2. The vertical force F_v.

$$F_v = -W_2 \cdot \cos(\alpha) + K_2 \cdot \cos(\alpha+\delta) - A \cdot \sin(\alpha) + W_3 \cdot \cos(\alpha) \tag{2.27}$$

If there is no cavitation the water pressures forces W_1 and W_2 can be written as:

$$W_1 = \frac{p_{1m} \cdot \rho_w \cdot g \cdot v_c \cdot e \cdot h_i^2 \cdot b}{(a_1 \cdot k_i + a_2 \cdot k_{max}) \cdot \sin(\beta)} \tag{2.28}$$

and

$$W_2 = \frac{p_{2m} \cdot \rho_w \cdot g \cdot v_c \cdot e \cdot h_i \cdot b}{(a_1 \cdot k_i + a_2 \cdot k_{max}) \cdot \sin(\alpha)} \tag{2.29}$$

For W_3 an empirical relation is found, namely:

$$W_3 = 0.3 \cdot \cot(\alpha) \cdot W_2 \tag{2.30}$$

With the limitation that W_3 can never be higher than W_2. This relation suffices well for blade angles between 30° to 60°. This sub-pressure behind the blade will be discussed in chapter 3.11. In case of cavitation W_1 and W_2 become:

$$W_1 = \rho_w \cdot g \cdot (z+10) \cdot h_i \cdot b / \sin(\beta) \tag{2.31}$$

and

$$W_2 = \rho_w \cdot g \cdot (z+10) \cdot h_b \cdot b / \sin(\alpha) \tag{2.32}$$

The effect of cavitation on the sub-pressure behind the blade is yet unknown. For the moment the above stated equation is used.

Wismer and Luth [80] in 1972 researched the inertia forces part of the total cutting forces. The following equation is derived:

$$T = \rho_g \cdot v_c^2 \cdot \frac{\sin(\alpha)}{\sin(\alpha+\beta)} \cdot h_i \cdot b \tag{2.33}$$

The cohesion and the adhesion can be determined with soil mechanical experiments. For the cohesion and adhesion forces the following equations are valid:

$$C = c \cdot h_i \cdot b / \sin(\beta) \tag{2.34}$$

and

$$A = a \cdot h_b \cdot b / \sin(\alpha) \tag{2.35}$$

The gravitation force (mass) follows from:

$$G = (\rho_s - \rho_w) \cdot g \cdot h_i \cdot b \cdot \frac{\sin(\alpha+\beta)}{\sin(\beta)} \cdot \left\{ \frac{(h_b + h_i \cdot \sin(\alpha))}{\sin(\alpha)} + \frac{h_i \cdot \cos(\alpha+\beta)}{2 \cdot \sin(\beta)} \right\} \tag{2.36}$$

This is in accordance with the area that is used for the water pressures calculations (see figure 2.4).

The flow resistance is included explicit in equation (2.24), although this term will have to be introduced as a boundary condition in the water pressures calculations. Since the flow resistance is proportional with the square of the cutting velocity, while the volume strain rate is proportional with the cutting velocity, it is impossible to include the flow resistance in the dimensionless water pressures calculations. It is proposed to include the flow resistance as an external force in the force equilibrium, according:

$$W_4 = C_w \cdot 0.5 \cdot \rho_w \cdot v_c^2 \cdot b \cdot \left(\frac{(h_b + h_i \cdot \sin(\alpha))}{\sin(\alpha)} + \frac{h_i \cdot \cos(\alpha+\beta)}{2 \cdot \sin(\beta)} \right) \tag{2.37}$$

In which the force W_4 has an angle χ with the direction of the velocity. The values of C_w and χ will have to be determined experimentally. The term behind the blade width b is in accordance with the cut layer, as is used in the water pressures calculations.

2.7 Determination of the shear angle β

In chapter 2.6 the equations are derived with which the forces on a straight blade can be determined according the method of Coulomb [76]. Unknown in these equations is the shear angle β.

In literature several methods are used to determine this shear angle.

The oldest is perhaps the method of Coulomb [76]. This method is widely used in sheet pile wall calculations. Since passive earth pressure is the cause for failure here, it is necessary to find the shear angle at which the total, on the earth, exerted force by the sheet pile wall is at a minimum.
When the water pressures are not taken into account, an analytical solution for this problem can be found.

Another failure criterion is used by Hettiaratchi and Reece [23]. This principle is based upon the cutting of dry sand. The shear plane is not assumed to be straight as in the method of Coulomb, but the shear plane is composed of a logarithmic spiral from the blade tip that changes into a straight shear plane under an angle of $45° - 0.5 \cdot \varphi$ with the horizontal to the sand surface. The straight part of the shear plane is part of the so-called passive Rankine zone. The origin of the logarithmic spiral is chosen such that the total force on the blade is minimal.

There are perhaps other failure criterions for sheet pile wall calculations known in literature, but these mechanisms are only suited for a one-time failure of the earth. In the cutting of soil the process of building up stresses and next the collapse of the earth, is a continuous process.

Another criterion for the collapse of earth, is the determination of those failure conditions for which the total required strain energy is minimal. Rowe [67] uses this principle for the determination of the angle under which local shear takes place. From this point of view it seems plausible to assume that those failure criterions for the cutting of sand have to be chosen, for which the cutting work is minimal. This implies that the angle of friction has to be chosen for which the cutting work and therefore the horizontal force, exercised by the knife on the soil, is minimal. Miedema [54,57] and Steeghs [72,73] have chosen this method.

Assuming that the water pressures are dominant in the cutting of packed sand, and thus neglecting adhesion, cohesion, gravity, inertia forces, flow resistance and sub-pressure behind the blade, the derivative of the force F_h (equation (2.26)) to the shear angle β becomes:

$$\frac{\partial F_h'}{\partial \beta} = -p_{1m} \cdot h_i \cdot \frac{\sin(\varphi) \cdot \sin(\alpha+2\cdot\beta+\delta+\varphi)}{\sin^2(\beta) \cdot \sin(\alpha+\beta+\delta+\varphi)} + p_{2m} \cdot h_b \cdot \frac{\sin(\delta)}{\sin(\alpha) \cdot \sin(\alpha+\beta+\delta+\varphi)}$$
$$+ \frac{\partial p_{1m}}{\partial \beta} \cdot h_i \cdot \frac{\sin(\varphi)}{\sin(\beta)} + \frac{\partial p_{2m}}{\partial \beta} \cdot h_b \cdot \left\{ \frac{\sin(\alpha+\beta+\varphi)}{\sin(\alpha)} - \frac{\sin(\alpha+\beta+\delta+\varphi)}{\sin(\alpha+\delta)} \right\} \tag{2.38}$$

With the following simplification:

$$\frac{\partial F_h'}{\partial \beta} = \frac{\partial F_h}{\partial \beta} \cdot \frac{\sin(\alpha+\beta+\delta+\varphi)}{\sin(\alpha+\delta)} \tag{2.39}$$

Since the value of the shear angle β, for which the horizontal force is minimal, has to be found, equation (2.38) is set equal to zero, so the simplification according equation (2.39) is allowed. It is clear that this problem has to be solved iterative, because an analytical solution is impossible.

The Newton-Rhapson method works very well for this problem. In tables 2.2 to 2.7 (see appendix B5) the resulting shear angles, calculated with this method, can be found for several values of δ, φ, α, several ratios of h_b/h_I and for the non-cavitating and cavitating cutting process.

Interesting are now the results if another method is used. To check this the shear angles have also been determined according Coulomb's criterion: there is failure at the shear angle for which the total force, exerted by the blade on the soil, is minimal. The maximum deviation of these shear angles with the shear angles according tables 2.2 to 2.7 (see Appendix B5) has a value of only 3° at a blade angle of 15°. The average deviation is approximately 1.5° for blade angles to 60°.

The forces have a maximum deviation of less than 1%. It can therefore be concluded that it does not matter if the total force, exercised by the soil on the blade, is minimized, or the horizontal force. Next these calculations showed that the cutting forces, as a function of the shear angle, vary only slightly with the shear angles, found using equation (2.38). This sensitivity increases with an increasing blade angle. Figure2.9 shows this for the following conditions:

$\alpha = 15°, 30°, 45°$ and $60°$, $\delta = 24°$, $\varphi = 42°$, $h_b/h_i = 1$ and a non-cavitating cutting process.

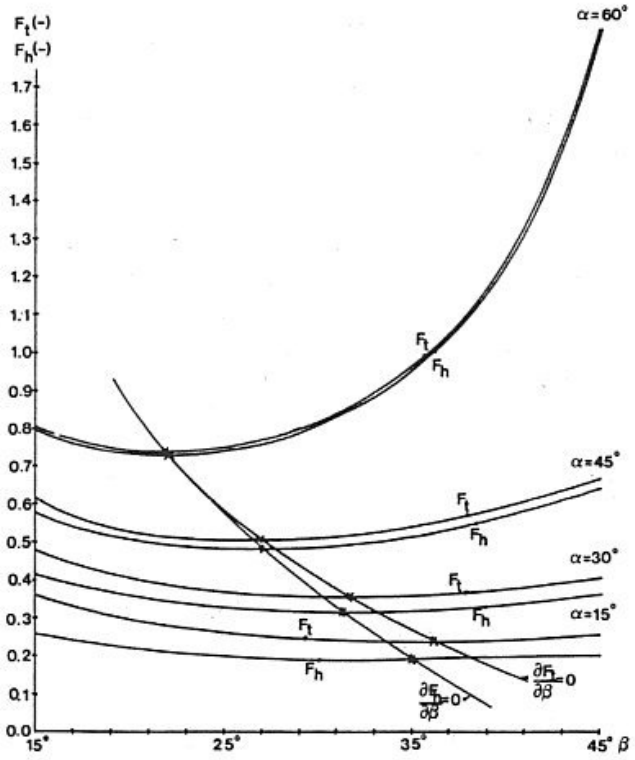

Figure 2-9 The forces F_h and F_t as function of the shear angle δ and as function of the blade angle α, determined by minimizing the specific cutting energy and minimizing the total cutting force F_t.

2.8 The coefficients a_1 and a_2

In the derivation of the calculation of the water sub-pressures around the blade, resulting in equations (2.28) and (2.29), it already showed that the water sub-pressures are determined by the permeability of the undisturbed sand and the permeability of the disturbed sand. Equation (2.15) of chapter 2.3 shows this dependence. The water sub-pressures are determined for several ratios of the initial permeability of the undisturbed sand to the maximum permeability of the disturbed sand:

$k_i/k_{max} = 1$

$k_i/k_{max} = 0.5$

$k_i/k_{max} = 0.25$

The average water sub-pressures p_{1m} en p_{2m} can be put against the ratio k_i/k_{max}, for a certain shear angle β. A hyperbolic relation emerges between the average water sub-pressures and the ratio of the permeabilities. If the reciproke values of the average water sub-pressures are put against the ratio of the permeabilities a linear relation emerges.

The derivatives of p_{1m} and p_{2m} to the ratio k_i/k_{max} are, however, not equal to each other. This implies that a relation for the forces as a function of the ratio of permeabilities can not be directly derived from the found average water sub-pressures.

This is in contrast with the method used by Van Leussen and Van Os [40]. In [40] it is assumed that the average pore pressure on the blade has the same dependability on the ratio of permeabilities as the average pore pressure in the shear zone. No mathematical background is given for this assumption.

For the several ratios of the permeabilities it is possible with the shear angles, determined in chapter 2.7, to determine the dimensionless forces F_h and F_v. If these dimensionless forces are put against the ratio of the permeabilities, also a hyperbolic relation is found (Miedema [57]), shown in figure 2.10.

A linear relation can therefore also be found if the reciproke values of the dimensionless forces are taken. This relation can be represented by:

$$1/F_h = a + b \cdot k_i / k_{max} \tag{2.40}$$

With the next transformations an equation can be derived for a weighed average permeability k_m:

$$a_1 = \frac{b}{a+b} \qquad a_2 = \frac{a}{a+b} \tag{2.41}$$

So:

$$k_m = a_1 \cdot k_i + a_2 \cdot k_{max} \quad \text{with:} \quad a_1 + a_2 = 1 \tag{2.42}$$

Since the sum of the coefficients a_1 en a_2 is equal to 1 only coefficient a_1 is given in the tables 2.8 to 2.13 (see appendix B5). It also has to be remarked that this coefficient is determined on the basis of the linear relation of F_h (dimensionless c_1), because the horizontal force gives more or less the same relation as the vertical force, but has besides a much higher value. Only for the 60° blade, where the vertical force is very small and can change direction, differences occur between the linear relations of the horizontal and the vertical force as function of the ratio of the permeabilities.

From table 2.8 to 2.13 (see Appendix B5) can be concluded, that the influence of the undisturbed soil increases when the blade-height/layer-thickness ratio increases. This can be explained by the fact that the water that flows to the shear zone over the blade has to cover a larger distance with an increasing blade height and therefore has to overcome a higher resistance. Relatively more water will have to flow through the undisturbed sand to the shear zone with an increasing blade height.

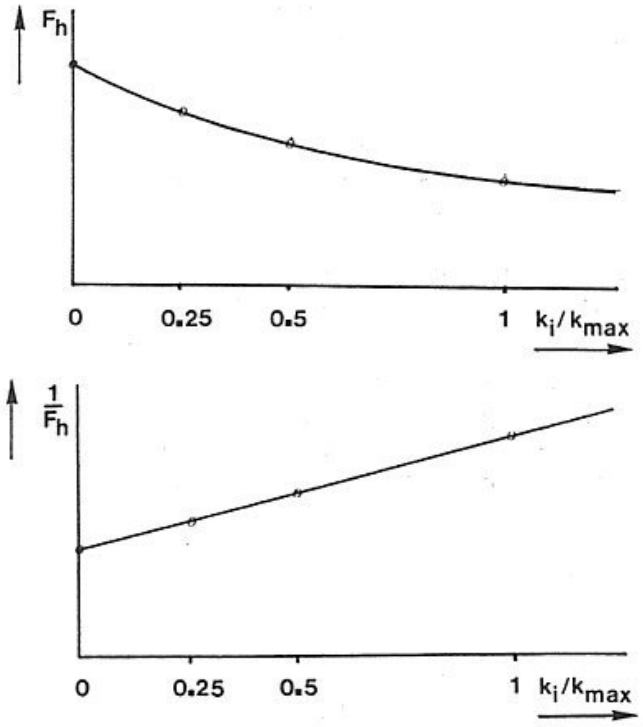

Figure 2-10 a, above: The force F_h as function of the ratio between the initial permeability k_i and the residual permeability k_{max}.
b, below: The reciproke of the force F_h as function of the ratio between the initial permeability k_i and the residual permeability k_{max}.

2.9 Determination of the coefficients c_1, c_2, d_1 and d_2.

If only the influence of the water sub-pressures on the forces that occur with the cutting of saturated packed sand under water is taken in to account , equations (2.26) and (2.27) can be simplified. It will be assumed that the non-cavitating process switches to the cavitating process for that cutting velocity v_c , for which the force in the direction of the cutting velocity F_h is equal for both processes.

In reality, however, there is a transition region between both processes, where locally cavitation starts in the shear zone. Although this transition region starts at about 65% of the cutting velocity at which, theoretically, full cavitation takes place, it shows from the results of the cutting tests that for the determination of the cutting forces the existence of a transition region can be neglected.

In the simplified equations the coefficients c_1 en d_1 represent the dimensionless horizontal force (or the force in the direction of the cutting velocity) in the non-cavitating and the cavitating cutting process. The coefficients c_2 and d_2 represent the dimensionless vertical force or the force perpendicular to the direction of the cutting velocity in the non-cavitating and the cavitating cutting process.

For the non-cavitating cutting process:

$$F_{ci} = c_i \cdot \rho_w \cdot g \cdot v_c \cdot h_i^2 \cdot b \cdot e / k_m \tag{2.43}$$

In which:

$$c_1 = \frac{\left(p_{1m} \cdot \frac{\sin(\varphi)}{\sin(\beta)} + p_{2m} \cdot \frac{h_b}{h_i} \cdot \frac{\sin(\alpha+\beta+\varphi)}{\sin(\alpha)} \right) \cdot \sin(\alpha+\delta)}{\sin(\alpha+\beta+\delta+\varphi)} - p_{2m} \cdot \frac{h_b}{h_i} \cdot \frac{\sin(\alpha)}{\sin(\alpha)} + p_{3m} \cdot \frac{h_b}{h_i} \cdot \frac{\sin(\alpha)}{\sin(\alpha)} \tag{2.44}$$

and,

$$c_1 = \frac{\left(p_{1m} \cdot \frac{\sin(\varphi)}{\sin(\beta)} + p_{2m} \cdot \frac{h_b}{h_i} \cdot \frac{\sin(\alpha+\beta+\varphi)}{\sin(\alpha)} \right) \cdot \sin(\alpha+\delta)}{\sin(\alpha+\beta+\delta+\varphi)} - p_{2m} \cdot \frac{h_b}{h_i} \cdot \frac{\cos(\alpha)}{\sin(\alpha)} + p_{3m} \cdot \frac{h_b}{h_i} \cdot \frac{\cos(\alpha)}{\sin(\alpha)} \tag{2.45}$$

And for the cavitating cutting process:

$$F_{ci} = d_i \cdot \rho_w \cdot g \cdot (z+10) \cdot h_i \cdot b \tag{2.46}$$

In which:

$$d_1 = \frac{\left(\frac{\sin(\varphi)}{\sin(\beta)} + \frac{h_b}{h_i} \cdot \frac{\sin(\alpha+\beta+\varphi)}{\sin(\alpha)}\right) \cdot \sin(\alpha+\delta)}{\sin(\alpha+\beta+\delta+\varphi)} - \frac{h_b}{h_i} \cdot \frac{\sin(\alpha)}{\sin(\alpha)} + p_{3m} \cdot \frac{h_b}{h_i} \cdot \frac{\sin(\alpha)}{\sin(\alpha)} \tag{2.47}$$

and:

$$d_2 = \frac{\left(\frac{\sin(\varphi)}{\sin(\beta)} + \frac{h_b}{h_i} \cdot \frac{\sin(\alpha+\beta+\varphi)}{\sin(\alpha)}\right) \cdot \cos(\alpha+\delta)}{\sin(\alpha+\beta+\delta+\varphi)} - \frac{h_b}{h_i} \cdot \frac{\cos(\alpha)}{\sin(\alpha)} + p_{3m} \cdot \frac{h_b}{h_i} \cdot \frac{\cos(\alpha)}{\sin(\alpha)} \tag{2.48}$$

The values of the 4 coefficients are determined by minimalising the cutting work, or that is at that shear angle β where the derivative of the horizontal force to the shear angle is zero (see chapter 2.7).
For the non-cavitating cutting process the coefficients c_1 and c_2 are given in the tables 2.14 t/m 2.25 (see appendix B5). For the cavitating cutting process the values of d_1 and d_2 are given in the tables 2.26 t/m 2.37 (see appendix B5). The coefficients c_1 , c_2 , d_1 en d_2 are given in these tables as functions of α, δ, φ and the ratio h_b/h_i.

The tables are printed for the case without sub-pressure behind the blade and for the case where the sub-pressure behind the blade is calculated according equation (2.30), according next list:

Tables 2.14 t/m 2.16: c_1 without sub-pressure behind the blade.
Tables 2.17 t/m 2.19: c_1 with sub-pressure behind the blade.
Tables 2.20 t/m 2.22: c_2 without sub-pressure behind the blade.
Tables 2.23 t/m 2.25: c_2 with sub-pressure behind the blade.
Tables 2.26 t/m 2.28: d_1 without sub-pressure behind the blade.
Tables 2.29 t/m 2.31: d_1 with sub-pressure behind the blade.
Tables 2.32 t/m 2.34: d_2 without sub-pressure behind the blade.
Tables 2.35 t/m 2.37: d_2 with sub-pressure behind the blade.

Equations (2.43) en (2.46) form the basis of the simplified analytical models for the cutterhead (chapter 4) and the cutter-wheel (chapter 5).

2.10 Determination of φ and δ from cutting tests

The soil/steel angle of friction and the angle of internal friction can be determined from cutting tests. Sand without cohesion or adhesion is assumed in the next derivations, while the mass of the cut layer has no influence on the determination of the soil/steel angle of friction. In figure 2.11 is indicated which on the blade acting forces have to be measured to determine the soil /steel angle of friction.

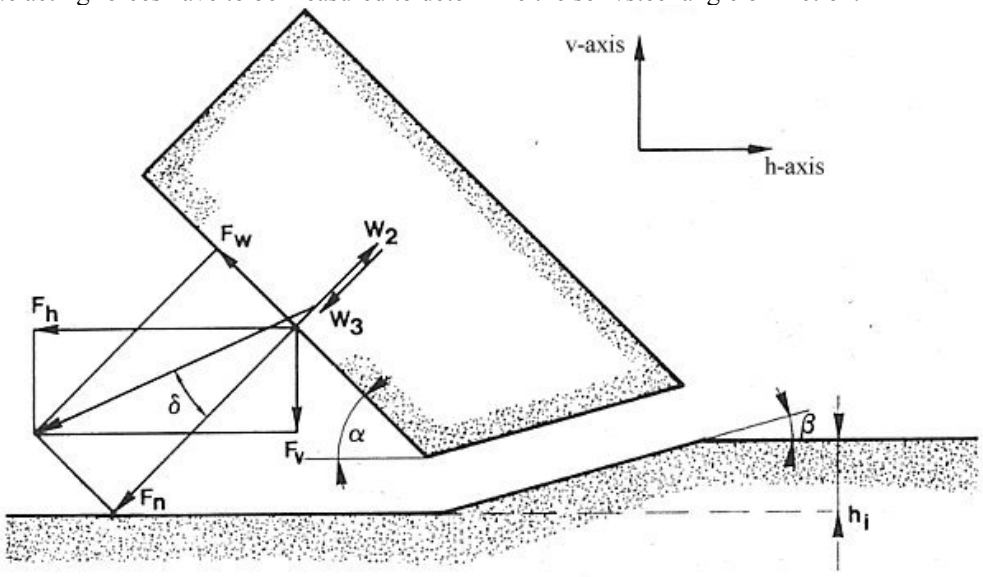

Figure 2-11 The forces from which the soil/steel angle of friction can be determined.

The forces F_h and F_v can be measured directly. Force W_2 results from the integration of the measured water pressures on the blade. Force W_3 will be discussed in chapter 3.11 (see also equation (2.30)). From this figure the normal force on the blade, resulting from the grain stresses on the blade, becomes:

$$F_n = W_2 - W_3 + F_h \cdot \sin(\alpha) + F_v \cdot \cos(\alpha) \tag{2.49}$$

The friction force, resulting from the grain stresses on the blade, becomes:

$$F_w = F_h \cdot \cos(\alpha) - F_v \cdot \sin(\alpha) \tag{2.50}$$

The soil/steel angle of friction now becomes:

$$\delta = \arctan\left(\frac{F_w}{F_n}\right) \tag{2.51}$$

Determination of the angle of internal friction from the cutting tests is slightly more complicated. In figure 2.12 is indicated which forces, acting on the cut layer, have to be measured to determine this angle. Directly known are the measured forces F_h and F_v, while the inertia force T has to be determined using equation (2.33). The mass of the layer G can be determined with equation (2.36). The force W_3 results from a relation derived in chapter 3.11 (equation (2.30)). The force W_4 has to be determined experimentally. From measurements it is however known (chapter 3) that this force can be neglected. The force W_1 is unknown and impossible to measure. However from the numerical water pressures calculations the ratio between W_1 and W_2 is known. By multiplying the measured force W_2 with this ratio an estimation of the value of the force W_1 can be obtained, so:

$$W_1 = \left(\frac{W_1}{W_2}\right)_{calc} . W_{2meas} \tag{2.52}$$

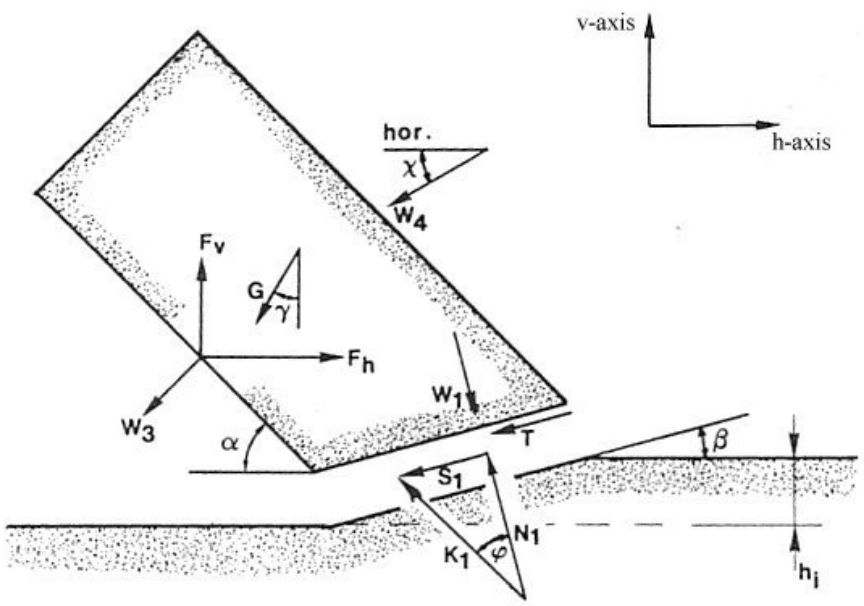

Figure 2-12 The forces from which the angle of internal friction of the sand can be determined.

For the horizontal and the vertical force equilibrium of the cut layer can now be written:

$$F_h - W_3 \cdot \sin(\alpha) = K_1 \cdot \sin(\beta+\varphi) - W_1 \cdot \sin(\beta) + T \cdot \cos(\beta) + G \cdot \sin(\gamma) + W_4 \cdot \cos(X) \tag{2.53}$$

and:

$$F_v - W_3 \cdot \cos(\alpha) = -K_1 \cdot \cos(\beta+\varphi) + W_1 \cdot \cos(\beta) + T \cdot \sin(\beta) + G \cdot \cos(\gamma) + W_4 \cdot \sin(X) \tag{2.54}$$

The angle of internal friction:

$$\varphi = \arctan\left(\frac{F_h - W_3 \cdot \sin(\alpha) + W_1 \cdot \sin(\beta) - T \cdot \cos(\beta) - G \cdot \sin(\gamma) - W_4 \cdot \cos(X)}{-F_v + W_3 \cdot \cos(\alpha) + W_1 \cdot \cos(\beta) + T \cdot \sin(\beta) + G \cdot \cos(\gamma) + W_4 \cdot \sin(X)}\right) - \beta \tag{2.55}$$

The derived equations (2.51) and (2.55) are used to determine the values of φ and δ from the performed cutting tests, which will be discussed in chapter 3.11.

2.11 The effect of a velocity component parallel to the blade edge

Important for the equilibrium of the cut layer is the soil/steel angle of friction, which acts in the plane perpendicular to the blade edge. It is assumed to be known that the friction force, occurring between two, in relation to each other, moving planes, acts in the direction of the velocity between the two planes. This implies that as a result of a velocity component parallel to the blade edge (sliding velocity) a friction force occurs parallel to the blade edge (sliding force) but in the opposite direction of the sliding velocity. If it is geometrically possible for the sand to move parallel to the direction of the blade edge, this can happen as a result of a velocity component parallel to the blade edge.

A known example of this phenomenon is the cutting process in a so-called “grader”. In figure 2.13 the involved velocity and force components are shown.

First the involved forces have to be known, before the acting forces can be discussed.

v_t The total velocity of the blade.
v_c The velocity component of the blade perpendicular to the blade edge.
v_r The relative velocity between the sand and the blade.
v_l The velocity component of the blade parallel to the blade edge.
f_0 The factor of v_l, with which the sand moves parallel to the blade edge.

In chapter 8 the determination of these three velocities is discussed extensively.

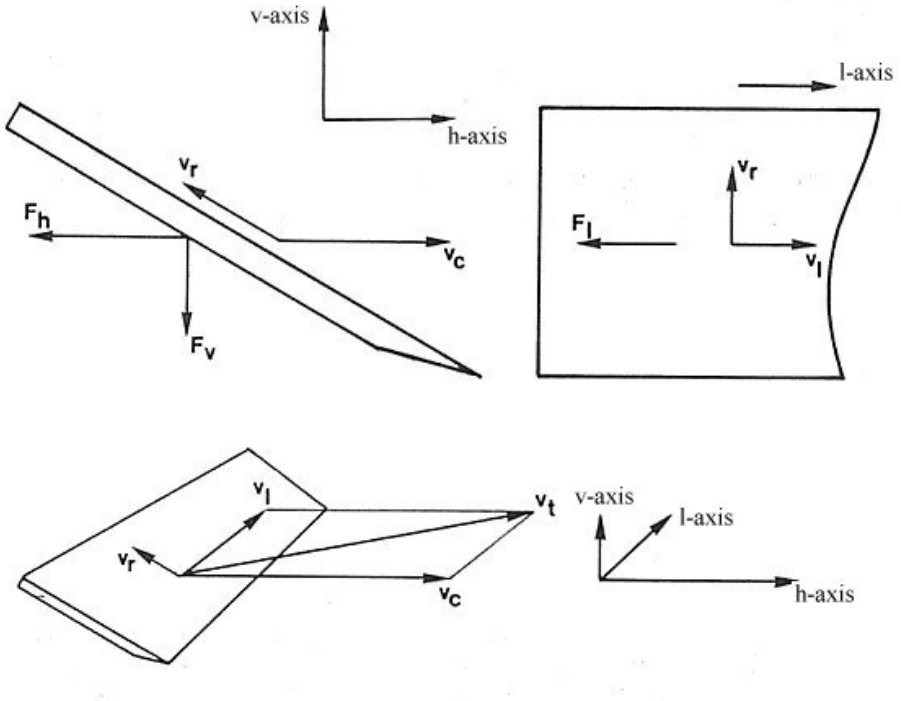

Figure 2-13 The velocity components and the force components on the blade.

The velocity components perpendicular and parallel to the blade edge are assumed to be known. The relative velocity between the sand and the blade perpendicular to the blade edge can be determined according:

$$v_r = v_c \cdot \frac{\sin(\beta)}{\sin(\alpha+\beta)} \tag{2.56}$$

For the effective soil/steel angle of friction in the plane perpendicular to the blade edge can now be written:

$$\delta_e = \mathrm{atn}\left(\frac{v_r}{\sqrt{\left(v_r^2 + v_l^2 \cdot (1-f_0)^2\right)}} \cdot \tan(\delta)\right) \tag{2.57}$$

In chapter 2.7 is discussed, that the shear angle β is dependent on the soil/steel angle of friction δ, which works in the plane perpendicular to the blade edge. However when there is a velocity component parallel to the blade edge, these angles become mutual dependent (equations (2.56) and (2.57)). An iterative solution for β and δ_e has to be found. Because the shear angle β is not very sensitive to changes in the soil/steel angle of friction δ_e a simple iteration, according figure 2.14, is sufficient.

With known α, h_i, h_b, δ, and φ, the friction force between the sand and the blade in the plane perpendicular to the blade edge can be determined with:

$$F_w = F_h \cdot \cos(\alpha) - F_v \cdot \sin(\alpha) \tag{2.58}$$

The friction force parallel to the direction of the blade edge, opposite to the direction of the velocity component parallel to the blade edge, can now be determined with:

$$F_l = F_w \cdot \frac{v_l \cdot (1-f_0)}{v_r} \tag{2.59}$$

In which f_0 represents the factor of the sliding speed that is forced upon the sand as a result of the sliding friction. The resistance of the sand against the acceleration in the sliding direction can be determined with:

$$F_l = \rho_g \cdot v_c \cdot h_i \cdot b \cdot v_l \cdot f_0 \tag{2.60}$$

Equating equations (2.59) and (2.60) gives the value for f_0:

$$f_0 = \frac{F_w}{\left(F_w + \rho_g \cdot v_c \cdot h_i \cdot b \cdot v_r\right)} \tag{2.61}$$

Because the inertia forces can be neglected, in the cutting of saturated packed sand, in comparison with the forces as a result of the water pressures, the factor f_0 is approximately 1. This implies that the force in the sliding direction of the blade is also negligible. This force becomes only substantial at very high cutting velocities. With this the components of the cutting force in the three directions (F_h, F_v and F_l) are known.

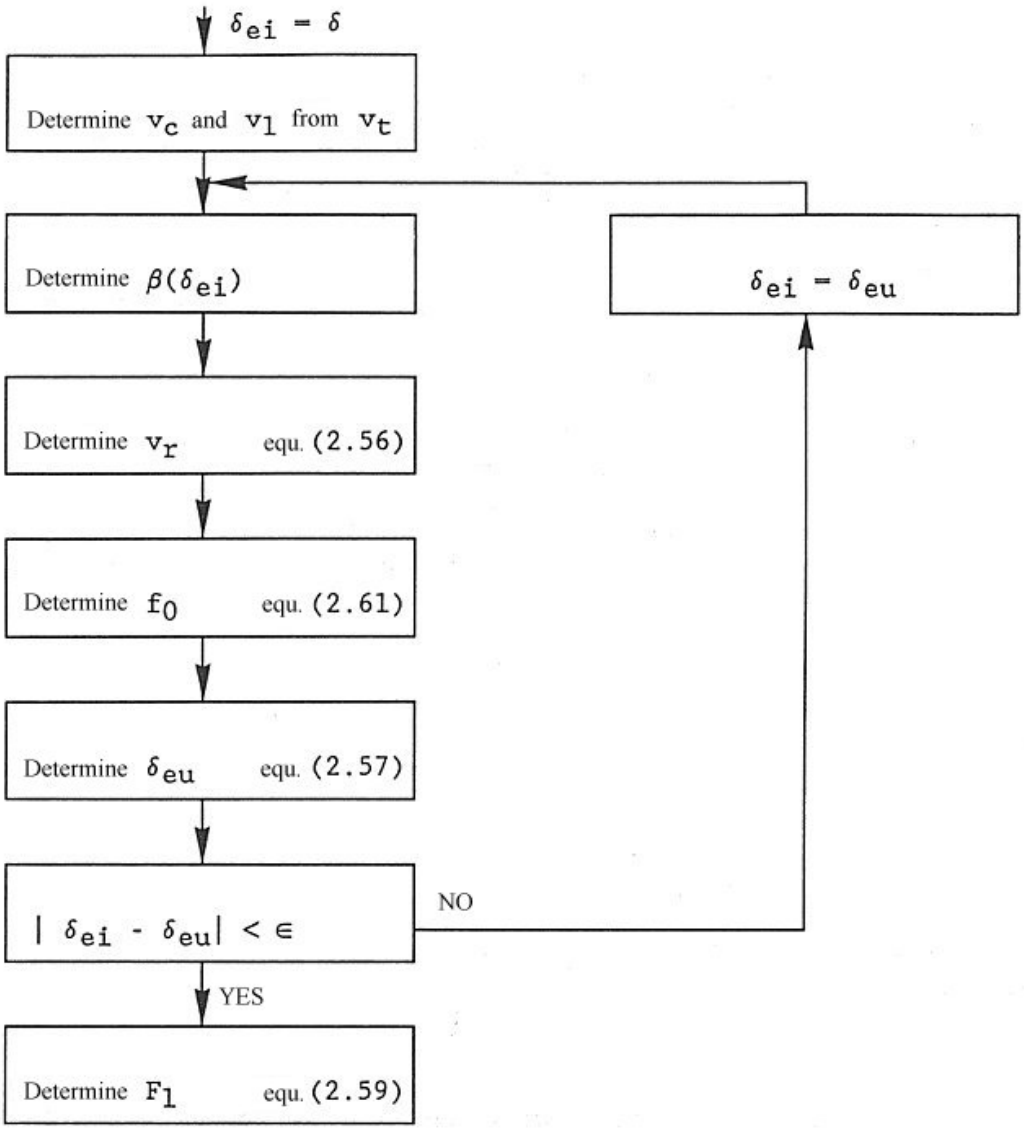

Figure 2-14 The determination of the effective soil/steel angle of friction δ_e and the sliding force F_l. Within the iteration an in-going effective angle of soil/steel friction δ_{ei} and an out-going effective angle of soil/steel friction δ_{eu} are used. When these two angles are equal qithin a certain accuracy $\in$ the effective angle of soil/steel friction is determined. With this the sliding force F_l can be determined from equation (2.59).

2.12 Wear and side effects

In the previous chapters the blades are assumed to have a reasonable sharp blade tip and a positive clearance angle. A two dimensional cutting process has also been assumed. In dredging practice these circumstances are hardly encountered. It is however difficult to introduce a concept like wear in the theoretical model, because for every wear stage the water pressures have to be determined numerically again.

Also not clear is if the assumption that the sand shears along a straight line will also lead to a good correlation with the model tests with worn blades. Only for the case with a sharp blade and a clearance angle of -1° a model test is performed. This is discussed in chapter 3.9.

It is however possible to introduce the wear effects and the side effects simply in the theory with empirical parameters. To do this the theoretical model is slightly modified. No longer the horizontal and the vertical forces are used, but the total cutting force and its angle with the direction of the velocity component perpendicular to the blade edge. Figure 2.15 shows the dimensionless forces c_1, c_2, en c_t for the non-cavitating cutting process and the dimensionless forces d_1, d_2 en d_t for the cavitating process. For the total cutting force can be written dimensionless:

non-cavitating cavitating

$$c_t = \sqrt{(c_1 \cdot c_1 + c_2 \cdot c_2)} \qquad d_t = \sqrt{(d_1 \cdot d_1 + d_2 \cdot d_2)} \tag{2.62}$$

For the angle that the force makes with the direction of the velocity component perpendicular to the blade edge:

$$\theta_t = \mathrm{atn}\left(\frac{c_2}{c_1}\right) \qquad \Theta_t = \mathrm{atn}\left(\frac{d_2}{d_1}\right) \tag{2.63}$$

It is proposed to introduce the wear and side effects according:

$$c_{ts} = c_t \cdot c_s \qquad d_{ts} = d_t \cdot c_s \tag{2.64}$$

and

$$\theta_{ts} = \theta_t \cdot \theta_s \qquad \Theta_{ts} = \Theta_t \cdot \Theta_s \tag{2.65}$$

For the side effects can now be written:

$$c_{tr} = c_t \cdot c_r \qquad d_{tr} = d_t \cdot c_r \tag{2.66}$$

and

$$\theta_{tr} = \theta_t \cdot \theta_r \qquad \Theta_{tr} = \Theta_t \cdot \Theta_r \tag{2.67}$$

In chapter 4 and 5 it will appear, that in particular the angle of rotation of the total cutting force as a result of wear, has a large influence on the force needed for the haul motion of cutter-suction and cutter-wheel dredgers. Figure 2.16 gives an impression of the expected effects of the wear and the side effects.

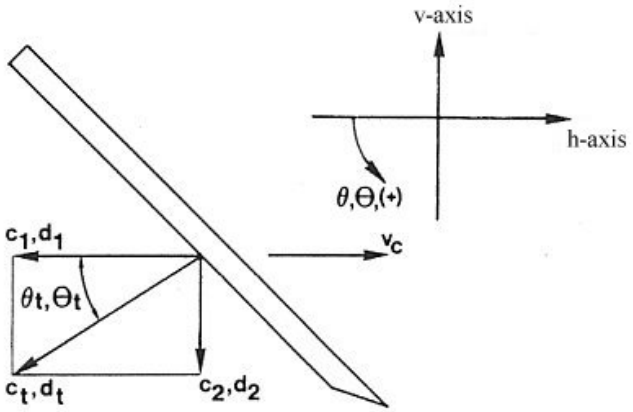

Figure 2-15 The total dimensionless cutting force c_t, d_t and the angle it makes with the velocity direction θ_t, ϑ_t, where this angle is positive when aimed downward.

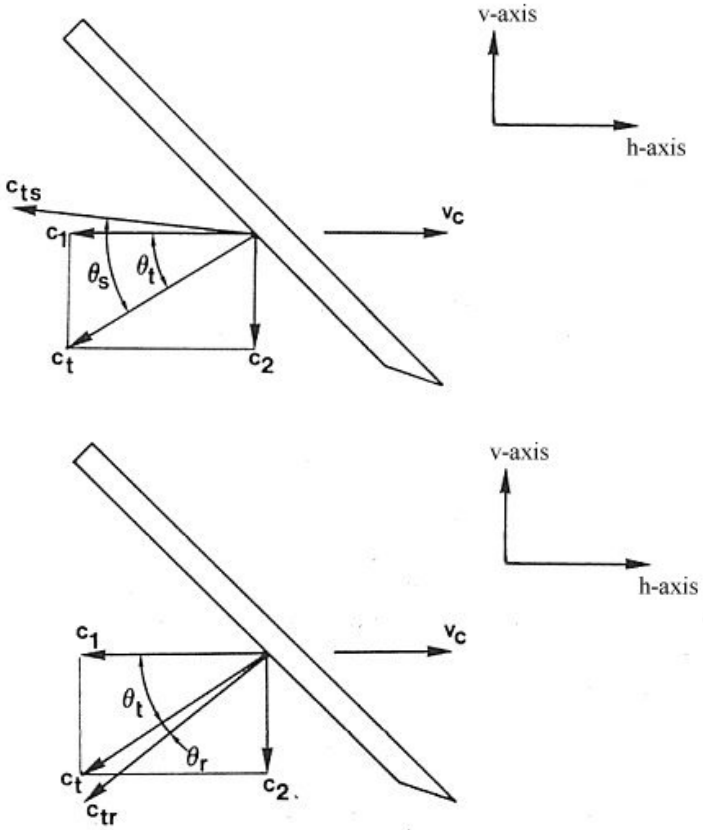

Figure 2-16 a, above: The influence of wear on the magnitude and the direction of the dimensionless cutting force c_t for the non cavitating cutting process.
b, below: The influence of side effects on the magnitude and the direction of the dimensionless cutting force c_t for the non cavitating cutting process.

2.13 Specific cutting energy

In the dredging industry, the specific cutting energy is described as:

The amount of energy, that has to be added to a volume unit of soil (e.g. sand) to excavate the soil.

The dimension of the specific cutting energy is: kN/m².

Adhesion, cohesion, gravity and the inertia forces will be neglected in the determination of the specific cutting energy. For the case as described in chapter 2, cutting with a straight blade with the direction of the cutting velocity perpendicular to the blade (edge of the blade), the specific cutting energy can be written:

$$E = \frac{F_h \cdot v_c}{h_i \cdot b \cdot v_c} = \frac{F_h}{h_i \cdot b} \tag{2.68}$$

The method, with which the shear angle β is determined in chapter 2.7, is therefore equivalent with minimizing the specific cutting energy, for a certain blade geometry and certain soil mechanical parameters. For the specific energy, for the non-cavitating cutting process, can now be derived from equations (2.43) and (2.68), that:

$$E_{gc} = c_1 \cdot \rho_w \cdot g \cdot v_c \cdot h_i \cdot \frac{e}{k_m} \tag{2.69}$$

For the specific energy, for the fully cavitating cutting process, can be written from equations (2.46) and (2.68):

$$E_{ca} = d_1 \cdot \rho_w \cdot g \cdot (z+10) \tag{2.70}$$

From these equations can be derived that the specific cutting energy, for the non-cavitating cutting process is proportional to the cutting velocity, the layer-thickness, the volume strain and inversely proportional to the permeability. For the fully cavitating process the specific cutting energy is only dependent on the water depth.

Therefore it can be posed, that the specific cutting energy, for the fully cavitating cutting process is an upper limit, provided that the inertia forces, etc., can be neglected. At very high cutting velocities, however, the specific cutting energy, also for the cavitating process will increase as a result of the inertia forces and the water resistance.

A change in the specific energy occurs when the forward velocity of the blade is not perpendicular to the blade edge (chapter 2.11). Figure 2.17 shows this situation. For the non-cavitating cutting process the force F_h is not dependent on the sliding velocity, when in equation (2.43) the total velocity of the blade and the projected blade width are substituted by the cutting velocity and the blade width. The direction of this force is perpendicular to the blade edge, so that, when neglecting the sliding force F_l, for the specific cutting energy can be derived:

$$E_{gc} = \frac{F_h \cdot v_c}{h_i \cdot b \cdot v_c} = \frac{F_h \cdot \cos(\iota)}{h_i \cdot b_{pr}} = c_1 \cdot \rho_w \cdot g \cdot v_t \cdot h_i \cdot \frac{e}{k_m} \cdot \cos(\iota) \tag{2.71}$$

In this equation the total velocity of the blade v_t is included, which gives a better impression of the specific cutting energy, although $v_t \cdot \cos(\iota)$ is equal to v_c. The specific cutting energy of the cavitating cutting process does not change under influence of a sliding velocity, so equation (2.70) is still valid. However, cavitation occurs for this case at a higher total velocity, since the velocity important for the cutting process (the perpendicular velocity v_c) is smaller than the total velocity v_t.

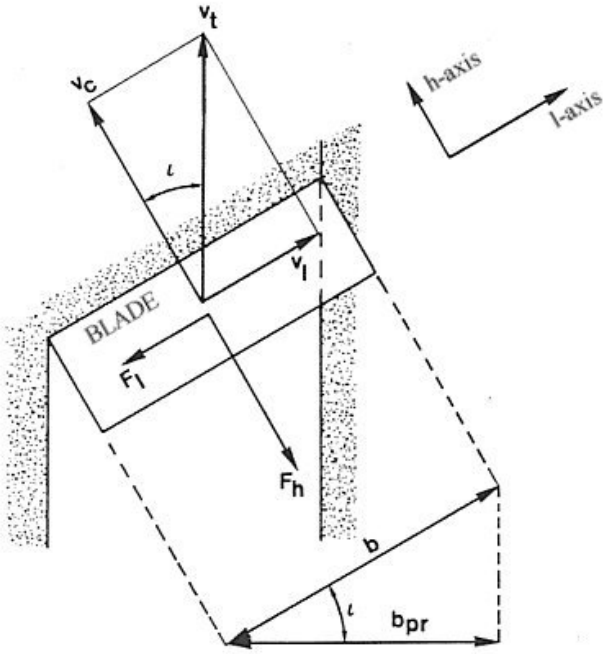

Figure 2-17 The velocity components v_t, v_c and v_l and the force F_h for a transverse component of the total blade velocity. Also the blade width b and the projected blade width b_{pr} from above.